

Application of Statistical Tests for Single-Level Populations to Neutron-Resonance-Spectroscopy Data*

H. I. Liou, H. S. Camarda,† and F. Rahn
Columbia University, New York, New York 10027

(Received 6 July 1971)

Dyson's new F -statistic test for spurious or missing levels has been applied to recent Er^{166} data and other of our results. The F test was shown to give good agreement with the Er^{166} total observed level set and our $l=0$ population choices for Er^{168} and Er^{170} , which were made before this test was known to us. The F test involves the evaluation, at each resonance position E_i , of a parameter F_i , defined as $F_i \equiv \sum_{j \neq i} f(x_{ji})$, where $x_{ji} = (E_j - E_i)/L$, and j is summed over all resonances between $(E_i - L)$ and $(E_i + L)$, and $f(x) = \frac{1}{2} \ln\{[1 + (1 - x^2)^{1/2}]/[1 - (1 - x^2)^{1/2}]\}$ for $x < 1$. The interval $L = M \langle D \rangle$ is characterized by a properly chosen integer, M . Dyson finds that $\langle F_i \rangle = n - \ln(n) - 0.656$, with a standard deviation of $[\ln(n)]^{1/2}$, where $n = \pi M$. If a spurious level is present, $\langle F_i \rangle = n$, evaluated at the spurious level. Thus, a large positive fluctuation occurs at a spurious level, while a low value of F_i results near a missed level. We have used the F test and other statistical tests to see if sets of $l=0$ resonances could be chosen for Th^{232} and U^{238} which agree with the Porter-Thomas (PT) distribution for $(\Gamma_n^0)^{1/2}$ and all statistical level-ordering tests. For the Th^{232} and U^{238} we used our older data for Γ_n^0 values and for the positions of the stronger s levels. Our more recent 1970 data for these isotopes were used to better establish the position of the weak levels. It should be emphasized that $\geq 80\%$ of the final choice s population is made of stronger s levels having Γ_n^0 values too large to be p levels. The only degree of freedom is for the s -level selection from the weaker $s+p$ levels observed. The number of weak "s" levels chosen is determined by the PT distribution and we attempt to fit (simultaneously) the Wigner nearest-neighbor spacing distribution, $\rho(S_j, S_{j+1}) \cong -0.27$, the Dyson-Mehta Δ statistic, and the Dyson F test. For both isotopes, good simultaneous fits were obtained. This result is highly unlikely unless the "true" s population satisfied the tests, since $\geq 80\%$ of the final choice involves nonweak s levels.

I. INTRODUCTION

The accompanying paper,¹ hereafter referred to as I, presents results of measurements of the neutron resonance levels for the target nuclei Er^{166} , Er^{167} , Er^{168} , and Er^{170} . In particular, the high quality and large statistical sample size of the Er^{166} data give by far the most conclusive evidence to date supporting orthogonal ensemble (O.E.) theories of long- and short-range order in single ($l=0$) population level spacings. In addition to the detailed analysis of that paper, this paper presents the results of an additional statistical test developed by Professor Freeman J. Dyson. We also give a new selection for the " $l=0$ populations" for neutron resonances in U^{238} and Th^{232} for ≤ 3 keV.

Theoretical predictions have evolved concerning the expected statistical properties of single, complete, s -level populations formed by the interaction of neutrons of ≤ 5 -20-keV energy with nuclei having average (s) level spacing $\ll 10$ keV, and thus a significantly large sample of levels in this energy interval. We consider the situation where intermediate-structure effects are absent, so that the *a priori* statistical mean values from which the population sample is drawn do not change signifi-

cantly over the interval. In our actual experimental studies of the interaction of neutrons with target nuclei where only neutron scattering or radiative capture is present, we usually do not have available *specific* tests to determine if each given observed weak resonance is of the main s -level population, or is a p level. When, as is usually the case, the observed level population structure has features, which show that it is a mixed s - and p - (or spurious "noise") level sample, we must rely on various statistical tests related to the expected properties of s and p populations to attempt to separate the s - from the p - (or spurious) level components. Such a separation is simple and obvious for the stronger levels of the observed sample. They can only be s levels, and, in favorable cases, they will form $\geq 80\%$ of the final s -population choice. The selection process can only be good in a statistical sense for the weak levels. If properly carried out, all but a small fraction of the assignments will be correct, but there is always a small probability that any given level assignment may be wrong.

When one wishes to obtain a "good" single s -level population for testing its compatibility with statistical theories, even-even spin-zero target nu-

clei are preferred. (Odd- A nuclei have $I \neq 0$ and two randomly intermixed s -level populations, corresponding to $J = I \pm \frac{1}{2}$.) The single-population properties relate to the measured parameters E_{0j} , Γ_{nj} , and $\Gamma_{\gamma j}$ for each level j . We are not concerned with the Γ_{γ} (capture) widths in determining if levels are s or p . A detailed high-resolution capture γ -spectroscopy study of the ratios of the intensities of strategically selected photon energies in the decay cascade seems to permit a reasonably unique choice of the J value for s levels in favorable odd- A cases. It may also prove to be able to provide a desired signature test distinguishing s and p levels. Since our own high-resolution studies do not include this technique, we are only concerned with the level energies and neutron-channel widths. The Γ_{nj} have an intrinsic $E_j^{1/2}$ energy dependence, so the "reduced" neutron width $\Gamma_{nj}^0 \equiv \Gamma_{nj}(1 \text{ eV}/E_j)^{1/2}$ is a more natural parameter to use. The distribution of the Γ_n^0 values about $\langle \Gamma_n^0 \rangle$ provides the first test, while the statistical aspects of the distribution of the population energies E_j provide the other tests. In principle, one can distinguish s and p levels from the angular distribution of the elastic scattering. However, the weak levels are not easily detected by *any* method, and they have $\sigma_{\text{scatt}} \ll \sigma_{\text{capture}}$, so such scattering angular-distribution studies are particularly difficult.

Test A. $\Gamma_n/\langle \Gamma_n^0 \rangle$ Distribution

It is now reasonably well established that the Porter-Thomas (PT), single-channel distribution law² should apply for members of a single s -level population over an energy interval which is not affected by intermediate-structure fluctuations. This formula can be written in the form

$$P(x) dx = (2/\pi)^{1/2} e^{-x^2/2} dx, \quad (1)$$

where $x = (\Gamma_n^0/\langle \Gamma_n^0 \rangle)^{1/2}$.

Usually the fit to Eq. (1) is excellent except at the lower end of the distribution where p or "noise" levels may be present in the observed population, or one or more weak s levels may have been missed. The *a priori* p -level density for an $I=0$ target is expected to be ≈ 3 times that for s levels ($2I+1$ factor), but, as discussed in I, the Γ_n values for p levels are expected to average smaller than for s levels by the energy-dependent factor $(S_1/S_0)(E/E_1)$. Here S_0 and S_1 are the s and p strength functions, E is the neutron energy of the level, and E_1 (≈ 350 keV for erbium) is the energy for which the neutron λ equals the nuclear radius R . The strength functions show optical-model size resonances where peaks of S_0 correspond to minima of S_1 , and vice versa. When the resolution of the neutron spectrometer is adequate,

more and more of the p levels are "detected" as the count period is extended for higher statistical accuracy. This can be a mixed blessing if one wishes to isolate the s -level population for comparison with statistical theories, since these p levels must then, somehow, be separated from the weak s levels. The problem is complicated by the fact that $\sim 8\%$ of the s levels have $\Gamma_n^0/\langle \Gamma_n^0 \rangle \leq 10^{-2}$, and 3% have $\leq 10^{-3}$. For studies covering an energy $\Delta E \sim 4$ keV, the (E/E_1) factor is $\sim 10^{-2}$ for much of the interval. It is, therefore, very helpful if S_0 is appreciably larger than S_1 , as occurs in the rare-earth region.

The main point of the comparison of all $(\Gamma_n^0)^{1/2}$ values with Eq. (1) is to see how many extra (or missing) weak levels are involved. See I for further discussion of this matter.

Test B. Nearest-Neighbor Level Spacing Distribution

Wigner first surmised in 1956 that there should be a repulsion between levels of a single population, and suggested the spacing distribution³ which bears his name,

$$P(y) dy = (\pi y/2) e^{-\pi y^2/4} dy, \quad (2)$$

where $y = S/\langle D \rangle$ is the adjacent level spacing in units of the population mean level spacing. When "extra" non- s levels are present, there tend to be too many small spacings.

Wigner related the problem of a single-population level distribution to that of the eigenvalue distribution of real, symmetric $N \times N$ square matrices having independent and random Gaussian-distributed matrix elements. Since his pioneering work, as discussed in I, many theorists have been intrigued by the problem and it has received much study and clarification. The present name for the various equivalent phrasings of the problem¹ is the O.E. The remaining statistical tests other than Eq. (2) discussed in this paper are based on the expected properties of the O.E.

Test C. Correlation Coefficient of Adjacent Nearest-Neighbor Level Spacings, $\rho(S_j, S_{j+1})$

This is expected to be ≈ -0.27 , with a statistical uncertainty which our Monte Carlo studies (described in I) show to be $\approx 0.92/(n)^{1/2}$ for n spacings if n is not too small.

Test D. Dyson-Mehta Δ Statistic (Ref. 4)

This is the mean square deviation of a best-fit straight line from the cumulative level count $N(E)$. The predicted values of $\langle \Delta \rangle$ and the standard deviation (S.D.), of Δ according to the O.E. theory are,

for n levels,

$$\langle \Delta \rangle = (1/\pi^2)[\ln(n) - 0.0687],$$

$$\text{S.D. of } \Delta = 0.11. \quad (3)$$

This predicted long-range "crystalline-like" ordering is quite dramatic, requiring $n \approx 20\,000$ for $\langle \Delta \rangle = 1.00$. Since the Wigner distribution, Eq. (2), is known to apply quite well for a single s -level population, the simplest "unbiased" alternative to the O.E. theory is an uncorrelated Wigner (U.W.) set of levels which are distributed as in Eq. (2), but with $\rho(S_j, S_{j+1}) = 0$ (intrinsic).

For a U.W. set, $\langle \Delta \rangle \approx n/55$ for not too small n . This is much larger than for the O.E. case for $n \geq 50$. The experimental value of Δ tends to be sensitive to incorrect level choices for the population, i.e., included p or spurious levels and/or missed weak s levels, in which case appreciably increased values of Δ usually result. Until our erbium results of I had been obtained, experimental Δ values tended to be much larger than predicted by Eq. (3). The Er¹⁶⁶ observed level set to 4.2 keV gives good agreement with tests A, B, C, and D. The Er¹⁶⁸ and Er¹⁷⁰ observed level sets to 4.7 or 4.8 keV show evidence from test A of an inclusion of partial p -level populations. The procedure used in I to distinguish s from p levels for Er¹⁶⁸ and Er¹⁷⁰ was mainly based on the use of a Bayes-theorem analysis. The resulting numbers of weak s levels were selected to agree with test A, but the resulting " s -level sets" also agreed with tests B, C, and D.

Other Tests

In addition to tests A, B, C, and D above, there are other statistical tests which were discussed in I and in the companion paper of Monahan and Rosenzweig.⁵ The statistic which we denote as $\sigma(k)$ was suggested by Bohigas and Flores (BF)⁶ for comparing data with their two-body random Hamiltonian ensemble (TBRE) theory, which they have investigated as a possible alternative to the O.E. theory. $\sigma(k)$ is the mean S.D. of the spacing of levels having k levels between them, in units of $\langle D \rangle$. The Er s populations agreed with the O.E. theory for this test, but not with their TBRE calculations (as is discussed in I).

The Monahan-Rosenzweig $\Lambda(n)$ statistic⁷ is applied to our Er data in an accompanying paper.⁵ The statistic is based on the feature of the O.E. theory that the cumulative nearest-neighbor spacing distribution has less mean square deviation from the integral form of Wigner distribution ($1 - e^{-\pi x^2/4}$) than would occur for a U.W. set.

Since our Er¹⁶⁶, and some other of our recent data, gave the first strong confirming test of the

Dyson-Mehta (DM) long-range order Δ statistic, as well as satisfying tests A, B, C, and D, we informed Professor Dyson and other interested theorists of our partial results before all analysis was finished. Professor Dyson was also interested in having his new " F " statistic⁸ (based on O.E. theory) applied to our data. This continuing discussion with Professor Dyson has led to an extensive series of computer studies of the over-all problem which forms the basis for the main contents of this paper.

In Sec. II, Dyson's F test is defined and a demonstration of how it is used is given. In Sec. III, the F statistic is applied to the erbium data. In Sec. IV, the F statistic and the other statistical tests mentioned above are applied to the earlier Th²³² and U²³⁸ published results⁹ (hereafter referred to as IX), where some use is made of more recent results for these elements. Until the recent Er¹⁶⁶ data were obtained, the thorium and uranium data provided the largest (many levels) sample of $l=0$, $J = \frac{1}{2}$ even-parity resonances belonging to a single population and have been used by theorists to test their theories.

Monahan and Rosenzweig⁷ applied their $\Lambda(n)$ statistic test to the old Columbia U²³⁸ results (IX), where many p -wave levels were present. They concluded that their test was fitted better by using *all* of the observed U²³⁸ levels than by the particular selection of $l=0$ levels made in IX. Since ~ 39 extra weak levels were observed, the implication from the Monahan-Rosenzweig test was that the previously chosen $l=0$ population, with its particular choice for excluded p -wave and spurious levels, was unsatisfactory. We have informed them of our new results so they can also apply their test to each of our final s -population selections as an extra, partially independent test.

II. F STATISTIC

Based on his circular O.E. theory, Dyson has developed an optimum statistic F to diagnose the presence of spurious or missing levels in an otherwise perfect sequence of levels. The F statistic defined below is applicable to single populations of levels. This represents another test in addition to those mentioned above. If single populations chosen from contaminated data are required to agree with all the different tests given above, a strong constraint is placed on the manner of selection. On the other hand, if a set of observed data agrees with all these tests, it is likely to be of high quality. All further remarks concerning sequences of levels will be in regard to single populations. This should be assumed throughout the remainder of this discussion.

For each level E_i in a series of observed levels, one calculates:

$$F_i = \sum_{j \neq i} f(x_{ji}), \quad \text{where} \quad x_{ji} = (E_j - E_i)/L, \quad (4)$$

where j runs through all levels between $(E_i - L)$ and $(E_i + L)$ excluding E_i , and

$$f(x) = \frac{1}{2} \ln \left[\frac{1 + (1 - x^2)^{1/2}}{1 - (1 - x^2)^{1/2}} \right] \quad \text{for } |x| < 1$$

$$f(x) = 0 \quad \text{for } |x| > 1. \quad (5)$$

$L = M\langle D \rangle$, $\langle D \rangle$ being the average level spacing and M an integer which is chosen arbitrarily. The expectation value of F_i and its S.D. for a true member of the series are

$$\langle F_i \rangle = n - \ln(n) - 0.656,$$

$$\text{S.D. of } F_i = [\ln(n)]^{1/2},$$

where $n = \pi M$. On the other hand, the expectation value of F_i for a spurious level E_i in an otherwise perfect sequence of levels is

$$\langle F_i \rangle = n \quad (\text{evaluated at the spurious level}).$$

This indicates that the presence of a spurious or missing level produces, on the average, a peak or a dip in F_i of magnitude $\sim \ln(n)$. This is to be

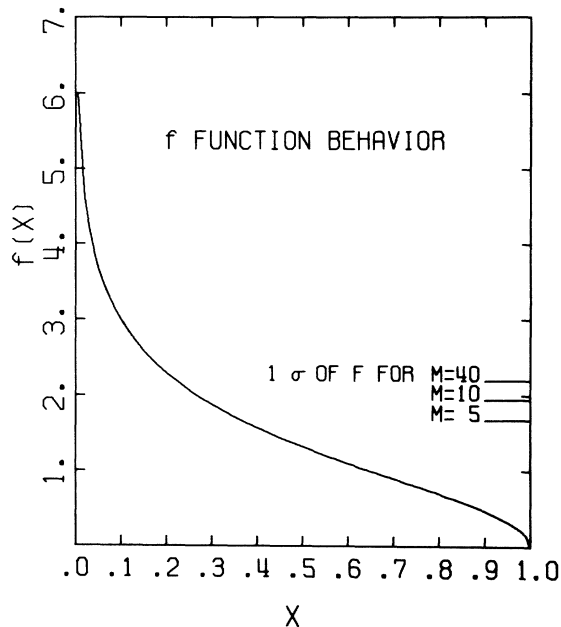


FIG. 1. Plot of the function $f(x) = \frac{1}{2} \ln \left\{ \frac{1 + (1 - x^2)^{1/2}}{1 - (1 - x^2)^{1/2}} \right\}$ vs x , where $F_i = \sum_j f(x_{ji})$. The theoretically predicted values of 1 standard deviation of F_i , for true levels, with $M=5, 10$, and 40 are shown on the right. It should be noted that a spurious level with a spacing $x \sim 0.05$ from a level being investigated will contribute to F , for that level, an amount equal to ~ 2 standard deviations ($M=10$).

compared with the natural scatter of F_i , $[\ln(n)]^{1/2}$, which is significantly smaller. Thus, it was hoped that one could identify regions where spurious levels were most likely present, or where a true level was missed.

The behavior of $f(x)$ vs x is shown in Fig. 1, and the S.D. of F_i for $M=5, 15$, and 40 is shown at the right. The test clearly gives decreasing but non-negligible weighting to levels having $|x| > 0.5$ or even > 0.8 .

The large value of $f(x)$ for very small x is not apt to be incorporated into the net F_i for a true population because of the level-repulsion factor. However, it is more likely to be included for a spurious level, where repulsion effects do not occur (except via limited instrumental resolution).

A spurious level clearly makes its largest contribution when F_i is evaluated at the position of the spurious level or at the nearest of the levels on either side. If the evaluation is made at the nearest true level, then the value of $|x|$ for the spurious level averages between zero, or some resolution limited value, to $\leq 1/2M$. The average value for $f(x)$ over this interval is $\ln M + 2 \ln 2 + 1$, which implies nearly the same net increase, as when F_i is evaluated at the spurious level. A missed true level has its largest effect when F_i is evaluated at the position of the nearest observed true level. In this case, the average "contribution" of $f(x)$ is $\cong -\ln(2M)$, which is a smaller negative effect than the positive one for a spurious level.

The transformed quantity G_i is easier to use, where $G_i = (F_i - \langle F_i \rangle) / (\text{S.D. of } F_i)$. The average G_i at a spurious level is $W = [\ln(n) + 0.656] / [\ln(n)]^{1/2}$. Since values of $G_i \geq 2.5$ have $\leq 1.2\%$ probability, we might see how W depends on M , and what M is needed for $W = 2.5$. This is an oversimplification, however, for while a spurious shift of only 2.5 is needed to make the net $G_i = 2.5$ when G_i starts from zero, the shift effect of the spurious component is superimposed on the "natural" fluctuations of G_i about zero. A spurious ΔG_i of 1 unit makes $G_i \rightarrow 2.5$ when the natural $G_i = 1.5$, but ΔG_i of 4.0 is needed if the natural $G_i = -1.5$.

Surprisingly, we find that the values of M required for W of 2, 3, and 4 units are, respectively, 4, 4600, and 750 000. The value of M required for W of 4, or even 3, is impossibly large for practical use in neutron spectroscopy. For $M \sim 12$, we find W is about 2.25. Consequently, for realistic choices of M the value of W is in the range 2.1 to 2.4. This is not large enough to give a net G_i as large as 2.5 units at a spurious level if the natural fluctuation is negative. As a result, it is difficult to be sure of a missed level unless the natural fluctuations reinforce the effect. However, the expected histogram of G_i values for a complete sin-

gle population may be sufficiently different from that of a "faulty" population such that contaminated data can be recognized.

Before comparing the data with the predictions of the F statistic, we will apply it to levels generated from the random-matrix model. This is useful in that one has complete control of the situation and a further feeling for the behavior of the F statistic can be gained.

As described in I, we have diagonalized 62 different 81×81 random matrices and have unfolded the density variation of the eigenvalues. The resulting sets of numbers simulate perfect data. The F test was applied to each of the 62 sets of these data. The results are presented in Fig. 2. The histogram (solid line) represents 2987 values of F ($M=14$) determined from the 62 sets of perfect data. The F values for the levels positioned less than a distance L from either end of the finite string of data were not included in the histogram. The smooth curve is a properly normalized Gaussian with the theoretically predicted average and variance of F_i .

As expected the agreement between the histo-

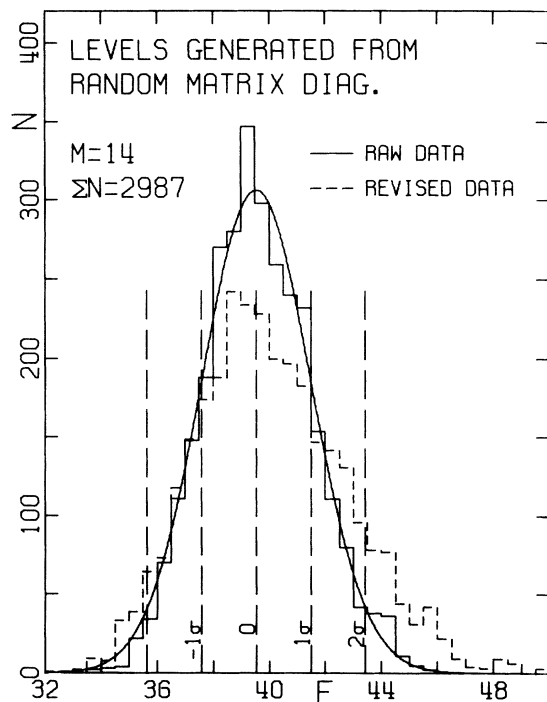


FIG. 2. Histograms of F_1 values found by applying the F statistic to simulated perfect data (solid line) generated by diagonalizing random matrices. The dashed histogram displays how the F distribution changes when the simulated perfect data are altered as described in the text. The smooth curve represents the theoretically expected behavior.

gram and the curve is excellent. The effect of adding two spurious levels and deleting two true levels for each set is shown by the dashed histogram. Note that the increase for a spurious level is greater than the decrease for a missed level, as expected.

Figure 3 shows the F values ($M=14$) vs the level energy for one of the above matrix diagonalizations (points indicated by open triangles). To test the sensitivity of the F statistic to a spurious or missing level, we removed the 20th level in the sequence and introduced a virtual level at the midpoint between the 54th and 55th level. The F test was then applied to this revised series of levels. The results are shown in Fig. 3 (points denoted by crosses). A comparison between the two plots shows that the influence of a spurious or missing level can be quite obvious under favorable circumstances.

This test was applied to each of the 62 sets of generated data with quite similar results in all cases. It should be noted, however, that on the average $\sim 5\%$ of the values of F_i for a perfect sequence of levels will lie 2 or more S.D. from the average value, and that the sensitivity for a *par-*

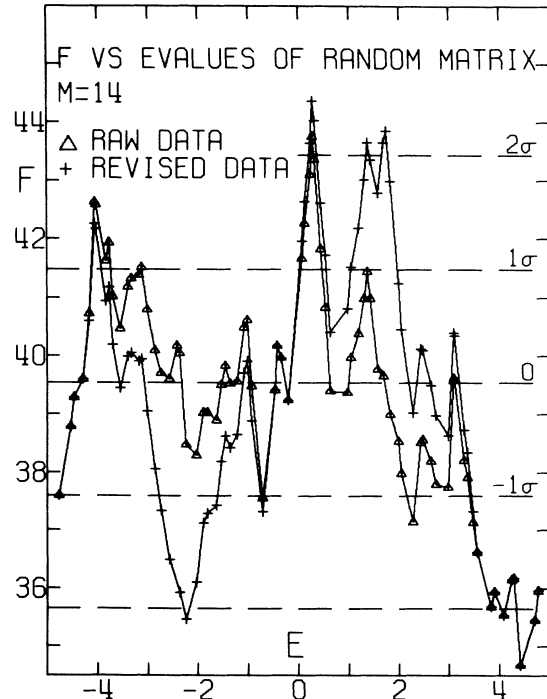


FIG. 3. Plot of successive values of F_1 for one set of random-matrix eigenvalues for which the semicircle-law eigenvalue density variation is unfolded. The eigenvalue scale is arbitrary and centered about 0.0. The open triangles represent the values before changes. The crosses indicate the altered eigenvalues as described in the text.

licular spurious or missing true level depends on whether or not the random fluctuation is aiding or opposing the effect.

III. F STATISTIC APPLIED TO THE ERBIUM DATA

The F statistic test was applied to both all observed Er^{166} levels, and to the particular "corrected" Er^{166} level set chosen in I. For this text, a value of $M = 10$ was chosen. The results are presented in Fig. 4. The histogram (solid line) represents the experimental G values of all observed Er^{166} levels to 4.2 keV, and the smooth curve represents the theoretical distribution. We see that the agreement is excellent. The additional agreement of the observed Er^{166} levels with the F statistic test provides further support for the validity of the O.E. theory, by showing that the F test also agrees with "good" data. The modified series of Er^{166} levels to 3 keV is also consistent with the F statistic as is seen in the dashed histogram in Fig. 4.

The PT and Wigner distributions using all observed Er^{168} and Er^{170} levels presented in I indicate that the observed levels contain a large number of p or spurious levels. Through the use of many tests, before we learned about the F statistic, $l=0$ populations for Er^{168} and Er^{170} were chosen as described in I. Here we will determine if

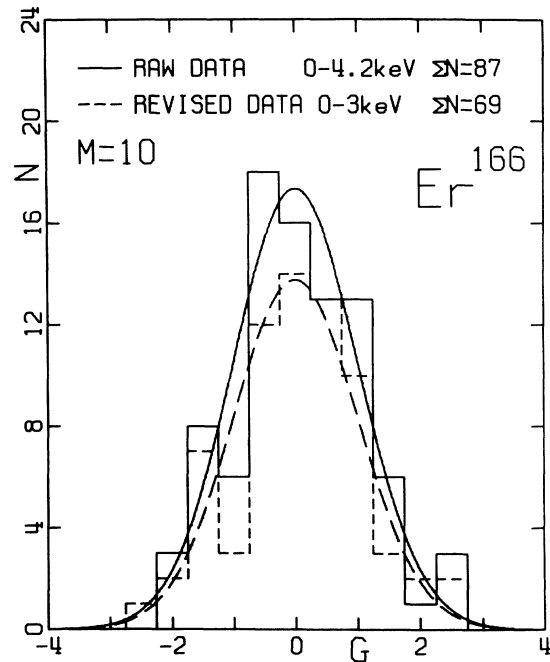


FIG. 4. Histograms of G values for the full observed Er^{166} level set (solid line) and the revised Er^{166} "s-level set" (dashed line), along with the theoretical predictions (smooth curves). The G values for the levels positioned less than a distance $M(D)$ from either the 0- or the 4.2-keV end of the full energy range are not included.

TABLE I. G values of Er^{168} calculated with $M = 10$. Levels for which G values are given in column 3 constitute the full observed population, while levels having entries in column 4 constitute the s -level selection of Paper I. P means that a level is chosen as p wave in Paper I. N indicates a level which was not observed but which is now included as being a "missed" s level. The G values for levels within ~ 10 levels of the beginning or end, labeled with *, were obtained by "reflecting" the level pattern about the first or last level of the set.

E_0 (eV)	$(\Gamma_n^0)^{1/2}$ (meV) ^{1/2}	G old	G new	E_0 (eV)	$(\Gamma_n^0)^{1/2}$ (meV) ^{1/2}	G old	G new	E_0 (eV)	$(\Gamma_n^0)^{1/2}$ (meV) ^{1/2}	G old	G new
79.7	2.22	7.32*	1.19*	1207.7P	0.27	2.84		2970.6	2.40	-1.44	-0.92
139.6P	0.10	9.15*		1342.8	0.49	1.40	-0.52	3027.4P	0.50	-1.76	
145.7P	0.07	9.28*		1356.3	2.95	1.31	-0.53	3095.3	3.42	-2.04	-1.20
174.3P	0.11	8.87*		1449.6	4.88	-0.65	-1.55	3165.8	1.95	-2.17	-1.38
188.9	2.40	8.58*	1.63*	1626.1	1.57	0.14	-1.43	3202.8P	0.39	-2.45	
244.4	5.93	7.11*	1.91*	1636.4P	0.33	0.08		3304.1	7.22	-3.51	-1.69
296.7P	0.13	6.94*		1681.3P	0.27	-0.75		3467.2	1.91	-4.16	-1.15
312.6	3.15	6.75*	1.60*	1713.9	1.26	-1.20	-1.14	3588.4	1.92	-3.10	-0.08
335.5P	0.22	5.71*		1810.7	2.32	-2.52	-0.55	3648.7	1.68	-2.35	0.58
410.8	0.31	4.18*	1.52*	1894.4	3.44	-2.48	0.01	3678.3	8.12	-2.33	0.62
446.0	0.33	3.55*	1.49*	1937.3	5.74	-2.53	0.00	3751.6	0.69	-2.35	0.19*
527.1	6.01	2.31*	0.70*	2044.6N			-0.49	3809.9	2.35	-2.28	-0.10*
587.3P	0.14	2.03*		2100.6P	0.42	-2.64		3849.9P	0.48	-2.56	
646.2N			-0.34*	2151.9	2.56	-2.26	-0.32	3997.7	1.32	-2.68	-0.35*
691.5P	0.20	1.45		2204.3	3.04	-2.30	-0.36	4098.3	6.73	-1.04*	0.30*
765.3	1.66	1.54	-0.76*	2325.9P	0.30	-2.06		4127.0P	0.45	-0.74*	
830.3	5.95	1.22	-1.06*	2364.1	5.65	-1.90	-0.88	4154.6	7.78	-1.01*	0.62*
985.7P	0.25	4.46		2456.6P	0.33	-0.93		4284.3	0.97	-1.42*	1.22*
990.6P	0.28	4.80		2472.4	1.49	-0.89	-0.41	4326.5	4.85	-1.37*	1.55*
1005.8	3.62	4.69	-1.35*	2544.0	0.76	-1.68	-0.34	4389.5	4.96	-1.46*	1.22*
1022.4P	0.23	4.29		2671.4	4.72	-0.50	0.44	4476.8P	0.46	-1.31*	
1093.9	5.51	4.33	-0.88	2682.7	6.66	-0.46	0.44	4515.6	2.54	-1.42*	0.87*
1106.1P	0.34	4.45		2814.2	1.65	-1.27	-0.39	4643.6	0.85	-0.50*	1.61*
1131.7	2.47	3.83	-1.05	2862.6	0.77	-0.87	-0.46	4671.1	3.29	-0.19*	2.00*
1193.2P	0.25	3.11		2900.5P	0.62	-0.95					

the chosen populations are consistent with the F test.

A value of $M = 10$ was chosen. The results are listed in Tables I and II, respectively, for Er^{168} and Er^{170} . The meaning of the symbols in these tables is explained in the table captions. In column 3 of Tables I and II, the F -test results using all observed Er^{168} and Er^{170} levels are presented. In both cases, the behavior of the experimental G values differs greatly from that expected for clean high-quality sample populations. The levels which were treated in I as comprising the s population for Er^{168} and Er^{170} are those for which G values are given in column 4. Note that added "missed" s levels in these selections have no G values shown in column 3. For both Er^{168} and Er^{170} , the experimental G values of column 4 are within the theoretical expectations for a good sequence of levels. This is in sharp contrast to the situation using all observed levels. This supports the conclusion that the method of the $l=0$ population selection used in I is satisfactory.

IV. SELECTION OF Th^{232} AND U^{238} $l=0$ SINGLE POPULATIONS

A. Th^{232}

The quality of the previously published Th^{232} data was examined by the application of many different statistical tests. The investigation was confined to the energy interval to 3.0 keV. The Th^{232} resonances reported in IX were in reasonable agreement with the PT distribution for a pure s population, so no corrected $l=0$ population choice was made at that time. The data were

found to be in agreement with the main trend of the Wigner distribution except for some fine structure superposed on the gross behavior. This is all quite apparent from the plots presented in IX. The more exacting tests, namely the Δ statistic and the F statistic, give strong evidence that the set of all levels is not consistent with the full predictions of the O.E. theory. The predicted value of Δ for the Th^{232} levels in the 3-keV region is 0.513 ± 0.11 . The experimental value of 0.917 is far from the theoretical value. The results of some of these tests are given below.

These tests indicate that the uncorrected Th^{232} level set of IX is not a high-quality pure $l=0$ single population of levels. Since the strengths of most resonances are much greater than those expected for p -wave levels, most of levels are clearly s wave and must be retained in any "corrected" population choice. It is only the weaker levels, which represent a small percentage of the total population, that are to be adjusted. In this respect, an inherent difficulty of the Th^{232} data (and of the U^{238} data) resides in the fact that any sample which is sufficiently thick to resolve most of the small s levels will also resolve many of the stronger p resonances, since in the region of the Periodic Table $A \sim 230-240$, $S_1 \approx S_0$. This problem is not as severe for rare-earth nuclei, where $S_0 > S_1$.

In order to help improve the selection of a proper Th^{232} s population (weak resonances), we made use of the more recent thorium data, which we obtained during a 1970 set of measurements and also referred to recent Saclay Th^{232} results.¹⁰ Our new thorium measurements were carried

TABLE II. G values of Er^{170} calculated with $M = 10$ (see the notes in Table I).

E_0 (eV)	$(\Gamma_p^0)^{1/2}$ (meV) ^{1/2}	G old	G new	E_0 (eV)	$(\Gamma_p^0)^{1/2}$ (meV) ^{1/2}	G old	G new	E_0 (eV)	$(\Gamma_p^0)^{1/2}$ (meV) ^{1/2}	G old	G new
95.1	9.50	2.62*	-0.40*	1524.0	1.35	1.16	-0.29*	3083.4P	0.60	-0.01	
164.6P	0.07	2.94*		1618.1P	0.29	0.72		3150.3P	0.52	-0.41	
221.9P	0.22	3.13*		1693.4P	0.38	0.90		3302.1	3.35	-0.28	-0.57*
284.0	5.84	3.01*	-0.59*	1827.6P	0.53	2.83		3352.8	0.97	0.11	-0.35*
394.3P	0.16	4.11*		1844.1	0.76	3.18	-0.46	3414.7P	0.76	0.31	
408.9P	0.25	4.26*		1874.9P	0.53	2.86		3464.4	1.82	0.41	-0.89*
483.8P	0.21	4.62*		1938.9P	0.38	2.37		3518.1P	0.35	0.17	
496.7	5.44	4.52*	-0.22*	2009.6	4.91	1.94	0.49	3599.7P	0.68	-0.54	
584.1P	0.31	4.04*		2087.2P	0.28	2.45		3698.0P	0.39	-0.69	
598.2	0.41	3.93*	0.05*	2101.1	5.53	2.43	0.79	3715.9	1.39	-0.89	-1.13*
698.2P	0.26	3.30*		2190.9	1.06	1.13	0.88	3843.9	2.20	-3.06	-0.84*
729.5P	0.29	3.56*		2249.3	6.69	0.98	0.65	4067.4P	0.38	-3.18*	
748.7	2.14	3.30*	0.17*	2291.0P	0.58	0.45		4123.6	2.37	-3.00*	0.49*
809.2P	0.18	1.94		2377.9	3.42	-0.57	-0.35	4193.3	4.27	-3.16*	1.15*
935.6	7.23	0.64	1.27*	2482.3P	0.53	-1.48		4240.9	4.55	-3.51*	1.11*
975.0	0.51	0.29	1.33*	2594.0	0.86	-2.27	-1.70	4318.8P	0.74	-4.31*	
1089.0	4.80	-1.14	0.83*	2830.6	9.15	-0.73	-1.76	4421.5	4.67	-5.16*	0.32*
1230.7	1.04	-1.64	0.27*	2857.3P	0.71	-0.39		4599.6	1.26	-5.37*	0.71*
1391.1	8.74	-0.43	0.05*	2928.0P	0.42	-0.08		4715.1	4.52	-5.14*	1.01*
1433.2P	0.28	0.16		2977.8	1.82	0.40	-1.80				
1512.1P	0.47	1.12		3018.6P	0.62	0.35					

out with a wider range of sample thicknesses (thickest $1/n \approx 12$ b/atom), a better signal-to-noise ratio, and much better statistical accuracy. As a result, many new weak levels were observed and some small levels previously claimed to exist were found to be spurious. This naturally led to a modified choice of *which* weak levels should be included in a new selection for the $l=0$ population.

The population selection procedure was as follows: We started by removing those weak levels of the old data which were not seen in the better quality new data and are thus regarded as being spurious (seven levels). It is tacitly assumed that in the more recent measurements essentially all s levels have been observed. In general, most of the larger of the newly observed weak levels were assigned to be s levels, as must be the case. The Γ_n^0 values have not yet been determined for the new data, but the relative strengths of all the weak levels could be determined to some extent from a simple inspection of the partially processed new data. Where very weak levels were assigned to be s , or where stronger weak levels were assigned to be p , the following considerations were emphasized.

The Wigner spacing distribution and the Δ statistic, which are sensitive to resonance positions and not to resonance strengths, were very helpful guides. In fact, the final choice of the s sample population was required to be consistent with PT theory, the Wigner spacing distribution, the expected value of $\rho(S_j, S_{j+1})$, the Δ statistic, and the F statistic.

The requirement of self-consistency for the selection with the many different tests places a strong constraint on the possible ways the choice of the weaker $l=0$ resonances can be made. There is no assurance of the existence of such a good fit solution involving just the selection of the weak $l=0$ population, unless the basic O.E. theory applies to the true $l=0$ population. No levels were used which had not been observed in our new thorium data. In addition, any weak level which was used was also observed recently at Saclay. As a result, we are confident that none of the levels added to the old Th^{232} data are spurious. The only question is one of s - or p -level assignment. The majority of s - and p -level assignments should be correct. However, a few individual assignments may be incorrect. It is mainly in a statistical sense that some confidence can be placed in the corrections made. These remarks also apply to the U^{238} level assignments. The self-consistency of the new $l=0$ population with the different tests is demonstrated below. Figure 5(a) shows the PT histogram for the new population choice along with the theoretical expectation (smooth curve). All of the new level choices appear in the lowest histogram box. A similar plot is shown in Fig. 5(b) for the nearest-neighbor spacing distribution. In Fig. 5(c), histograms of the experimental G values for both the old data and for the new population choice are presented, along with the theoretical predictions. In Table III for Th and

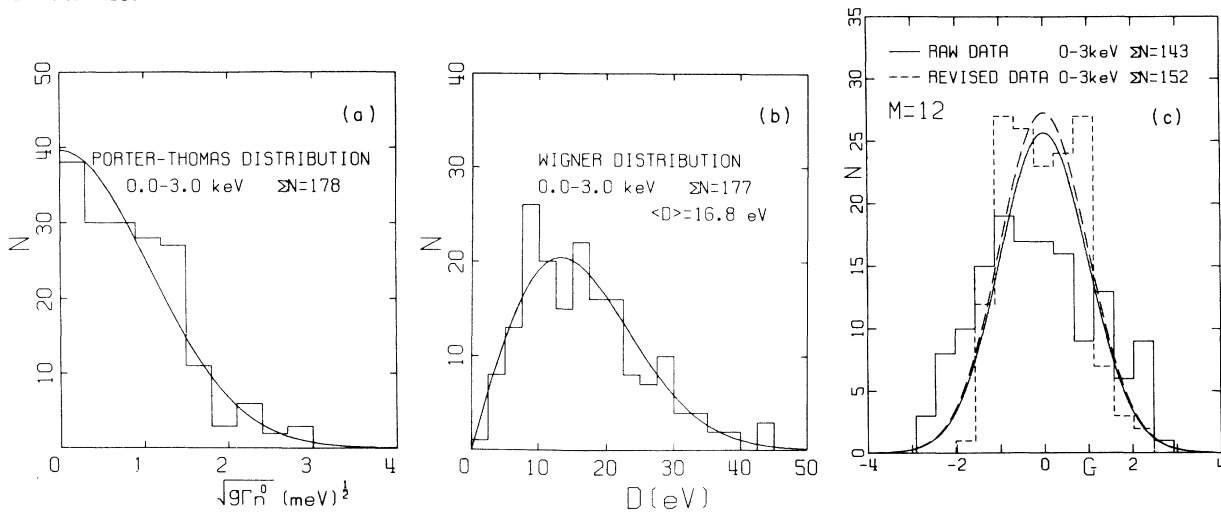


FIG. 5. (a) Histogram of the reduced neutron widths $(\Gamma_n^0)^{1/2}$ ($g=1$) for the newly selected Th^{232} $l=0$ population. The Porter-Thomas theory is represented by the smooth curve. (b) Histogram of adjacent level spacings for the newly selected Th^{232} $l=0$ population. The smooth curve represents the Wigner distribution. (c) Histograms of G values found for the full Th^{232} level set (solid line) of IX and our new $l=0$ population selection (dashed line). The theoretically expected behavior is represented by the smooth curves.

TABLE III. G values of Th^{232} calculated with $M=12$. The levels for which G values are given in column 3 represent the former (Paper IX) s -level population choice, while column 4 indicates the new s population choice. P denotes a level observed previously which is chosen as p in this paper. Any assigned p level which was not formerly observed is not included in this table. N signifies a newly found level which is assigned as s . F indicates a "level" previously thought to be real but now believed to be spurious. D indicates a formerly unresolved doublet at 1930.6 eV. The meaning of * is the same as in Table I. Those levels which are too strong to be p levels are labeled with a † next to their $(\Gamma_n^0)^{1/2}$ values.

E_0 (eV)	$(\Gamma_n^0)^{1/2}$ (meV) ^{1/2}	G old	G new	E_0 (eV)	$(\Gamma_n^0)^{1/2}$ (meV) ^{1/2}	G old	G new	E_0 (eV)	$(\Gamma_n^0)^{1/2}$ (meV) ^{1/2}	G old	G new
21.84	0.62†	4.40*	0.92*	1010.7	2.17†	-1.17	-1.31	1987.7	1.10†	-0.78	-1.31
23.48	0.81†	4.04*	0.55*	1039.5	0.67†	-1.22	-1.77	2004.9	0.75†	-0.33	-1.53
59.55	0.77†	1.61*	-1.92*	1065.8	0.32†	-0.46	-0.86	2015.2P	0.22	-0.22	
69.20	2.26†	1.56*	-1.90*	1077.4	0.60†	-0.17	-0.33	2034.8	0.28	-0.37	-0.96
112.90	1.06†	2.89*	-1.18*	1093.1	0.35†	0.15	-0.06	2051.3	0.59†	-0.11	-0.25
120.73	1.30†	3.79*	-0.86*	1110.1	0.92†	0.30	1.01	2061.5	0.98†	-0.16	0.00
128.00P	0.10	4.67*		1114.2N			1.17	2073.1	0.39†	-0.16	0.38
129.08	0.55†	4.63*	-1.06*	1122.4	0.20†	0.37	0.61	2078.3	0.60†	-0.36	0.34
145.92P	0.05	3.31*		1139.1	0.64†	0.76	-0.28	2097.4N			-0.46
154.34	0.10	3.16	-1.02*	1150.8	0.84†	1.17	-0.97	2116.6	1.20†	-2.06	-1.09
170.40	2.11†	2.93*	-0.63*	1156.7F	0.17	0.94		2147.6	1.22†	-1.71	-1.09
192.56	1.04†	3.61*	0.74*	1194.2	0.40†	0.62	-0.99	2162.8	1.34†	-1.39	-0.64
196.00	0.16	3.84*	1.13*	1204.5	0.17	0.77	-0.55	2178.0	1.22†	-1.12	-0.53
199.19	0.88†	3.45*	0.79*	1227.8	0.79†	1.42	-0.18	2196.3	1.05†	-1.05	-0.16
220.98	1.45†	1.26*	-0.90*	1243.3	0.65†	2.25	0.60	2216.2	0.50†	-0.80	0.54
251.29	1.41†	0.21	-1.01	1248.7	1.45†	2.19	0.59	2221.9	1.18†	-0.93	0.71
263.18	1.08†	0.14	-0.94	1269.5	0.69†	1.42	-0.16	2233.7N			0.05
285.61	1.29†	-0.57	-0.88	1292.2	1.30†	1.18	-0.07	2270.2	0.45†	-0.79	0.09
305.27	1.22†	-0.83	-0.65	1301.8	0.99†	1.08	-0.24	2276.1	0.92†	-0.61	0.16
328.75	1.95†	-1.12	-0.38	1334.7	0.26†	1.54	0.00	2286.6	2.14†	-1.01	-0.21
341.90	1.40†	-1.30	0.02	1345.5P	0.14	2.16		2321.5	0.35†	-0.56	0.03
365.06	1.21†	-1.17	0.85	1355.0	1.22†	2.55	1.45	2335.4	1.34†	-0.12	0.90
369.31	1.20†	-1.17	0.90	1359.8	0.32†	2.38	1.82	2344.6N			1.14
391.90N			1.10	1372.6N			2.17	2352.5	0.77†	0.34	0.94
400.82	0.71†	-2.30	1.22	1377.9	0.97†	1.74	2.17	2362.6F	0.32	0.67	
411.28N			1.27	1387.0	0.20	1.78	1.69	2374.6	1.28†	0.77	0.98
420.70	0.10	-2.45	0.94	1397.7	1.41†	1.35	0.91	2381.6	0.39†	0.67	1.01
454.34	0.20†	-1.85	0.67	1416.6F	0.14	0.48		2389.6	0.20	-0.12	0.49
462.42	1.70†	-1.73	0.88	1426.9	1.28†	0.33	0.08	2418.1	1.18†	-1.73	-1.08
476.64N			0.90	1433.6	0.92†	-0.20	-0.09	2439.4	0.32†	-2.15	-1.08
488.61	1.64†	-1.49	0.68	1461.4N			-1.03	2456.1	1.70†	-2.34	-1.03
510.68	0.47†	-0.60	0.50	1478.7N			-1.19	2478.8N			-0.95
528.57	0.84†	0.44	0.75	1509.5	0.24†	-1.49	-0.64	2491.6	0.20†	-2.64	-0.76
534.75P	0.10	0.84		1518.4	1.69†	-0.80	-0.19	2508.7	2.24†	-2.45	-0.80
540.10	0.17	0.47	0.59	1524.1	1.64†	-0.84	-0.33	2526.1	1.00†	-2.39	-0.89
569.89	1.02†	-0.40	1.44	1555.6	0.35†	-1.22	-1.41	2548.5N			-0.73
573.50N			1.69	1581.2	0.50†	-0.39	-0.94	2563.1	2.00†	-1.67	-0.25
578.19	0.28†	-0.55	1.31	1589.0	2.28†	-0.29	-0.76	2568.4	1.00†	-1.57	-0.41
598.17	0.61†	-1.10	-0.24	1603.0	0.97†	-0.43	-1.03	2611.9	1.07†	-0.73	-0.50
617.93	0.39†	-1.48	-1.02	1630.7	2.74†	0.20	-0.49	2622.9	0.32†	0.05	0.03
656.79	1.36†	-0.49	-0.03	1640.7	1.00†	0.47	-0.33	2634.0	1.58†	0.30	0.18
665.19	0.87†	-0.12	0.35	1660.9	1.38†	1.49	-0.00	2654.6	0.24	0.96	0.70
675.19	2.83†	-0.21	0.51	1672.3F	0.20	2.19		2664.0	1.73†	1.23	0.91
687.40	1.55†	-0.31	0.25	1677.8	0.68†	2.12	0.38	2677.2	0.45†	1.35	0.78
700.96	0.77†	-0.57	0.06	1697.0N			0.92	2688.7	1.67†	1.34	0.52
712.83	1.10†	-1.08	-0.39	1705.5	0.35†	1.89	1.09	2713.7	1.07†	1.71	0.62
740.80	2.83†	-2.57	-1.18	1720.1	0.85†	2.23	0.62	2721.5	0.35†	1.82	0.80
764.30N			-0.92	1728.2F	0.20	2.32		2733.2	2.41†	1.55	0.36
778.74	0.63†	-2.81	-1.13	1739.8	0.39†	2.09	1.10	2747.0	0.39†	1.33	-0.32
804.42	2.65†	-2.10	-0.62	1746.8	0.79†	1.88	1.12	2763.8F	0.24	1.34	
821.61	0.14	-1.70	0.06	1763.0	1.36†	0.73	0.60	2772.9	0.99†	1.10	-0.95
836.70N			0.87	1785.3N			0.36	2793.1	1.50†	0.51*	-0.64*
842.70	0.97†	-0.97	1.10	1803.3	1.22†	0.24	0.76	2815.5	0.63†	0.45*	-0.27*
850.82	0.14	-0.87	0.66	1811.7	0.97†	0.52	0.94	2832.0	0.71†	0.30*	0.46*
866.71	0.71†	-1.24	-0.51	1823.5	1.30†	0.19	0.52	2838.9N			0.52*
890.30	1.05†	-0.94	-1.15	1848.6	0.22	0.37	0.41	2852.8	1.66†	-0.17*	-0.04*
897.20F	0.10	-0.87		1853.8	0.89†	0.45	0.54	2882.3	0.49†	0.00*	-0.46*
906.57	0.24†	-1.33	-1.28	1861.5	0.82†	-0.17	-0.14	2895.1	0.50	0.21*	-0.29*
927.62N			-0.97	1900.7	1.48†	-1.83	-1.44	2914.4	0.40	0.08*	-0.37*
943.65	1.10†	-1.76	-0.87	1928.5N	0.37†		-0.27	2947.1	1.18†	1.13*	0.83*
963.05	0.45†	-1.18	-0.71	1930.6D	0.65	-1.90		2955.9	0.76†	1.77*	1.54*
983.05	0.97†	-0.67	-0.55	1931.7N	0.47†		-0.23	2964.8	0.62†	1.90*	1.81*
990.71	1.55†	-0.69	-0.64	1950.5	1.34†	-1.78	-1.20	2978.1	0.45	1.90*	1.87*
				1970.8	1.87†	-1.26	-1.28	2989.3	0.77†	1.94*	2.02*

TABLE IV. G values of U^{238} calculated with $M=12$. Levels having entries in column 3 constitute the full observed population in Paper IX, while column 4 indicates the new s population choice. The symbols P, F, N, *, and † have the same meaning as in Table III. Q indicates that a level was chosen to be p or spurious in Paper IX.

E_0 (eV)	$(\Gamma_n^0)^{1/2}$ (meV) ^{1/2}	G old	G new	E_0 (eV)	$(\Gamma_n^0)^{1/2}$ (meV) ^{1/2}	G old	G new	E_0 (eV)	$(\Gamma_n^0)^{1/2}$ (meV) ^{1/2}	G old	G new
6.68	0.77†	4.36*	0.90*	1000.3P	0.20	7.29		1974.6	3.24†	-7.45	-0.81
Q10.20P	0.02	4.00*		1011.2	0.24	7.91	0.87	2023.6	2.12†	-6.61	-0.76
21.00	1.38†	2.77*	0.83*	1023.0	0.45†	8.61	1.24	2031.1	1.05†	-6.29	-0.73
36.70	2.27†	1.60*	0.54*	1029.1	0.32†	8.86	1.10	2070.0N			-0.55
66.30	1.76†	1.12*	0.44*	Q1033.2P	0.14	8.61		2088.6	0.55†	-3.29	0.25
80.77	0.48†	1.44*	0.40*	1053.9	1.52†	7.66	0.05	2096.5	0.47†	-2.79	0.22
Q90.00P	0.09	1.44*		1068.1P	0.14	8.62		2124.3	0.32†	-1.54	0.12
102.78	2.55†	0.80*	0.15*	Q1070.5P	0.10	8.71		2145.9	0.87†	0.41	0.84
116.93	1.82†	0.01*	-0.14*	Q1081.1P	0.14	8.10		2152.8	1.95†	1.00	0.74
145.80	0.26†	-1.24*	-0.70*	Q1094.8P	0.14	8.52		2172.0P	0.22	1.77	
165.54	0.52†	-1.67*	-0.79*	1098.3	0.67†	8.65	0.56	2186.0	2.79†	2.57	0.70
190.34	3.30†	-2.18*	-0.94*	Q1102.3P	0.14	8.23		Q2194.0F	0.22	3.12	
208.65	1.97†	-2.52*	-1.05*	1108.9	0.95†	7.03	0.65	2201.4	1.55†	3.03	0.92
237.40	1.34†	-2.03	-1.04*	1131.4	0.24	4.69	1.09	2230.0	0.32	3.98	1.79
Q242.88P	0.10	-2.04		1140.4	2.55†	4.02	1.09	2235.7	0.32	4.41	1.92
Q263.94	0.12	-2.13	-0.70	1167.5	1.53†	2.44	1.15	Q2241.5F	0.17	4.31	
273.74	1.23†	-2.32	-0.63	1177.6	1.36†	1.99	1.22	2259.1	1.17†	4.45	2.10
291.11	0.95†	-2.86	-0.98	1195.0	1.63†	0.80	1.09	2266.4	1.75†	4.48	2.05
311.12	0.24†	-3.64	-1.37	1210.9	0.51†	-0.26	0.77	2281.3	1.52†	4.23	1.24
347.92	2.10†	-3.84	-1.68	1245.1	2.55†	-1.10	0.56	2288.7P	0.22	4.07	
376.92	0.24†	-3.36	-1.18	1267.0	0.87†	-0.91	0.96	Q2302.0F	0.14	3.14	
397.56	0.55†	-2.73	-0.54	1273.2	0.89†	-1.05	0.81	2315.9	0.55†	2.41	0.87
410.23	0.97†	-2.61	-0.45	1298.4	0.28†	-2.32	0.33	2337.4	0.32	1.55	1.20
434.19	0.63†	-2.09	-0.41	1317.2	0.33†	-3.00	0.42	2352.0	1.14†	1.43	1.72
Q454.17	0.14	-1.59	-0.03	1335.7	0.17	-3.20	0.23	2356.0	1.14†	1.21	1.63
463.31	0.49†	-1.32	-0.01	1363.0N			-0.23	2392.5	0.48†	-1.16	0.55
478.70	0.37†	-1.42	-0.46	1393.0	1.92†	-1.01	0.25	2410.2	0.30	-1.26	0.56
Q488.89P	0.14	-1.60		1405.1	1.43†	0.59	0.62	2426.5	1.28†	-1.37	0.51
518.59	1.38†	-1.80	-0.80	Q1410.0P	0.17	1.09		2446.2	1.50†	-1.76	0.38
535.49	1.26†	-1.18	-0.54	Q1417.0P	0.17	1.42		2454.0	0.22	-2.11	0.10
Q556.05	0.14	-0.84	-0.39	1419.6	0.50†	1.40	0.72	2489.8	1.05†	-3.85	-1.21
580.20	1.06†	-0.05	-0.09	1427.7	0.89†	0.35	0.45	2520.7	0.45†	-3.86	-1.19
595.15	1.83†	0.46	-0.08	1444.1	0.75†	-0.93	-0.44	2548.7	2.61†	-2.99	-0.42
619.94	1.07†	1.90	0.32	1473.8	1.43†	-2.32	-1.43	2559.3	2.07†	-2.77	-0.23
Q623.53P	0.13	2.20		1523.1	2.35†	-1.04	-1.14	2580.7	2.19†	-2.45	-0.39
628.67	0.40†	1.79	0.20	1532.0	0.22	-0.46	-0.95	2598.7	3.32†	-1.59	-0.57
661.18	2.12†	1.16	-0.56	Q1546.0P	0.14	0.24		Q2604.0F	0.22	-1.43	
Q677.00P	0.14	1.73		1550.0	0.17	0.23	-1.08	2620.6	0.89†	-1.98	-0.64
693.23	1.14†	2.22	0.15	1565.0	0.22	-0.56	-1.25	2631.6	0.14	-2.36	-0.85
708.46	0.84†	3.10	0.56	1598.2	2.83†	-1.19	-1.69	2672.8	1.84†	-2.84	-1.35
721.80	0.22	4.04	0.82	1622.9	1.45†	-1.01	-1.38	2695.6	0.67†	-2.24	-1.07
Q730.10P	0.17	4.99		1638.2	1.00†	-0.46	-1.32	2716.8	1.17†	-1.39	-0.60
732.26	0.22	5.02	0.54	Q1645.4P	0.14	-0.32		Q2730.0	0.22	-0.99	-0.32
Q742.95P	0.14	3.94		1662.1	2.00†	-0.75	-1.69	2750.1	0.87†	-0.62	-0.23*
765.05	0.49†	3.32	0.43	1688.3	1.38†	-0.72	-1.63	2761.9	0.55†	-0.53	-0.30*
779.14	0.24	3.23	0.71	Q1700.7F	0.14†	-0.34		2787.9	0.45†	0.29*	-0.67*
790.88	0.42†	2.82	0.57	1709.4	1.16†	-0.46	-1.35	Q2798.0P	0.22	0.83*	
821.58	1.43†	2.81	0.19	1723.0	0.57†	-1.05	-1.39	2806.2	0.36	0.77*	-0.90*
Q846.62P	0.14	4.90		1744.0P	0.20	-2.06		2828.6	0.41†	0.69*	-1.38*
851.02	1.38†	5.46	0.98	1755.8	1.22†	-2.79	-1.36	Q2845.2F	0.22	1.01*	
856.15	1.66†	5.38	1.14	1782.3	3.32†	-3.50	-1.12	2866.1	1.22†	1.81*	-1.17*
866.52	0.37†	4.83	0.61	1797.7	0.22	-3.82	-0.74	2882.9	3.13†	2.48*	-1.01*
Q891.29P	0.17	5.08		1808.3	0.63†	-4.56	-0.99	2897.8	0.71†	3.18*	-1.07*
905.11	1.22†	6.33	0.04	1845.6	0.56†	-6.80	-1.23	Q2908.5P	0.22	3.48*	
909.90P	0.17	6.53		1868.0N			0.10	2923.6P	0.28	3.65*	
925.18	0.53†	6.56	0.44	1870.0N			0.06	2932.3	0.68†	3.73*	-1.16*
Q932.50P	0.10	6.84		1902.3	0.69†	-7.93	-1.12	2956.3	0.53†	3.98*	-0.58*
936.87	2.19†	6.54	0.50	1917.1	0.71†	-8.24	-1.15	2967.4	0.39†	4.58*	-0.53*
958.43	2.26†	5.37	-0.00	1953.0N			-1.05	Q2974.0F	0.22	4.75*	
991.78	3.32†	6.65	0.18	1968.7	3.61	-7.56	-0.58	2987.4	0.32	4.70*	-0.63*

Table IV for U^{238} are listed the G values obtained for all levels reported in IX and for our new s -population choices. The levels reported in IX are those for which G values are given in column 3. The new s -level selections are those levels for which G values are given in column 4. The symbol N appearing to the right of the level energy means the level was not observed in IX, but was observed in the new data and is selected to be an s level. The symbol F is attached to a level claimed to exist in IX but now believed to be spurious. Any level from IX which is now treated as being p , has the symbol P to the right of its level energy. Newly seen levels which are treated as p levels are not included in the table. With the higher quality of the more recent data, the thorium level at 1930.6 eV, previously reported to be a single level, was shown to be a doublet. The symbol D next to this level energy signifies this. A close examination of Table III will show specifically how the original data were altered. As shown in summary Table V, the old and new values for the Δ statistic are 0.917 (expected value 0.513) and 0.391 (expected value 0.518), respectively. Similarly, the old and new values of $\rho(S_j, S_{j+1})$ are -0.197 ± 0.077 and -0.204 ± 0.073 , where the expected value is ≈ -0.27 . Finally, the new best estimate of $\langle D \rangle$ for thorium is 16.8 eV for s levels with $\approx 0.6\%$ statistical uncertainty if our n choice is correct, but $\sim 2\%$ over-all including the uncertainty in value of n for the interval.

The agreement of the new s -population choice with all these tests is partially due to the use of these tests as a method of adjusting the choice of the $l=0$ weak levels. However, the chance of such good agreement with all of the tests is expected to be quite small unless the stronger levels, labeled with † in Tables III and IV, which provide a main "backbone" for the final selection and constitute $\approx 80\%$ of the final population choice, were distributed according to the O.E. theory. The existence of such a simultaneous solution is nontrivial and unlikely unless the true s population behaved in accord with the various theories.

B. U^{238}

The U^{238} level set reported in IX was also investigated for 0–3 keV. The statistical tests (the Δ , F , and Λ statistics) were applied to the old U^{238} level set (i.e., all observed levels) and also to the chosen $l=0$ population (i.e., excluding 33 levels designated as most likely p or spurious). The tests indicated that neither set of levels exhibited the behavior expected of a pure s population. Some of the results of the tests for the full U^{238} level sets and for selected U^{238} $l=0$ population of IX are shown in Table V and Fig. 6(c). At the time IX was written, there was no compelling experimental evidence in support of the longer-range level ordering predicted by O.E. theory. It is not surprising that the selected $l=0$ population of IX was unable to satisfy the powerful and more complete set of tests available now. The present course in choosing a new $l=0$ population is to start with all observed U^{238} levels in Paper IX supplemented by the more recent Columbia U^{238} data, and to utilize all the statistical tests presently available as the guide in the selection process.

The disagreement of the full U^{238} level set with the statistical tests was not unexpected because the U^{238} sample employed in the old measurements was sufficiently thick to observe most of the s resonances and, for reasons mentioned in the section on thorium, many strong p levels. This is an important difference between the old uranium and thorium measurements. Thorium had a lack of small levels and uranium had an excess of small levels. This means that altering the U^{238} data consisted mainly in removing from the observed level population small levels which are most likely p wave or spurious.

While all the tests were important, the F statistic and the Δ statistic were particularly useful for our new U^{238} s -level selection. When applied to the full U^{238} level set, the F statistic had many high values [see Fig. 6(c)] and a much larger range of values than expected for an O.E. set.

TABLE V. Summary of results for the tests of Δ and $\rho(S_j, S_{j+1})$ applied to Th^{232} and U^{238} resonances to 3 keV.

	Δ (exp)	Δ (theory)	$\rho(S_j, S_{j+1})$
Th^{232} full level set of IX	0.917	0.513	-0.197 ± 0.077
Th^{232} $l=0$ set of this paper	0.391	0.518	-0.204 ± 0.073
U^{238} full level set of IX	9.746	0.516	-0.006 ± 0.076
U^{238} $l=0$ set of IX	2.147	0.495	-0.261 ± 0.085
U^{238} $l=0$ set of this paper	0.417	0.497	-0.255 ± 0.081

For the Δ statistic, the effect of the extra levels was to increase the scatter of $\langle D \rangle$ over short energy intervals, thereby increasing the experimental value of Δ significantly.

The new U^{238} data from the 1970 Columbia run did not play a prominent role in the selection of

a new $U^{238} l=0$ population, because almost all the newly observed weak levels are believed to be p levels. It was useful, however, in locating the few marginally visible levels in IX which turn out to be spurious on the basis of the much higher statistical accuracy of the new measurements.

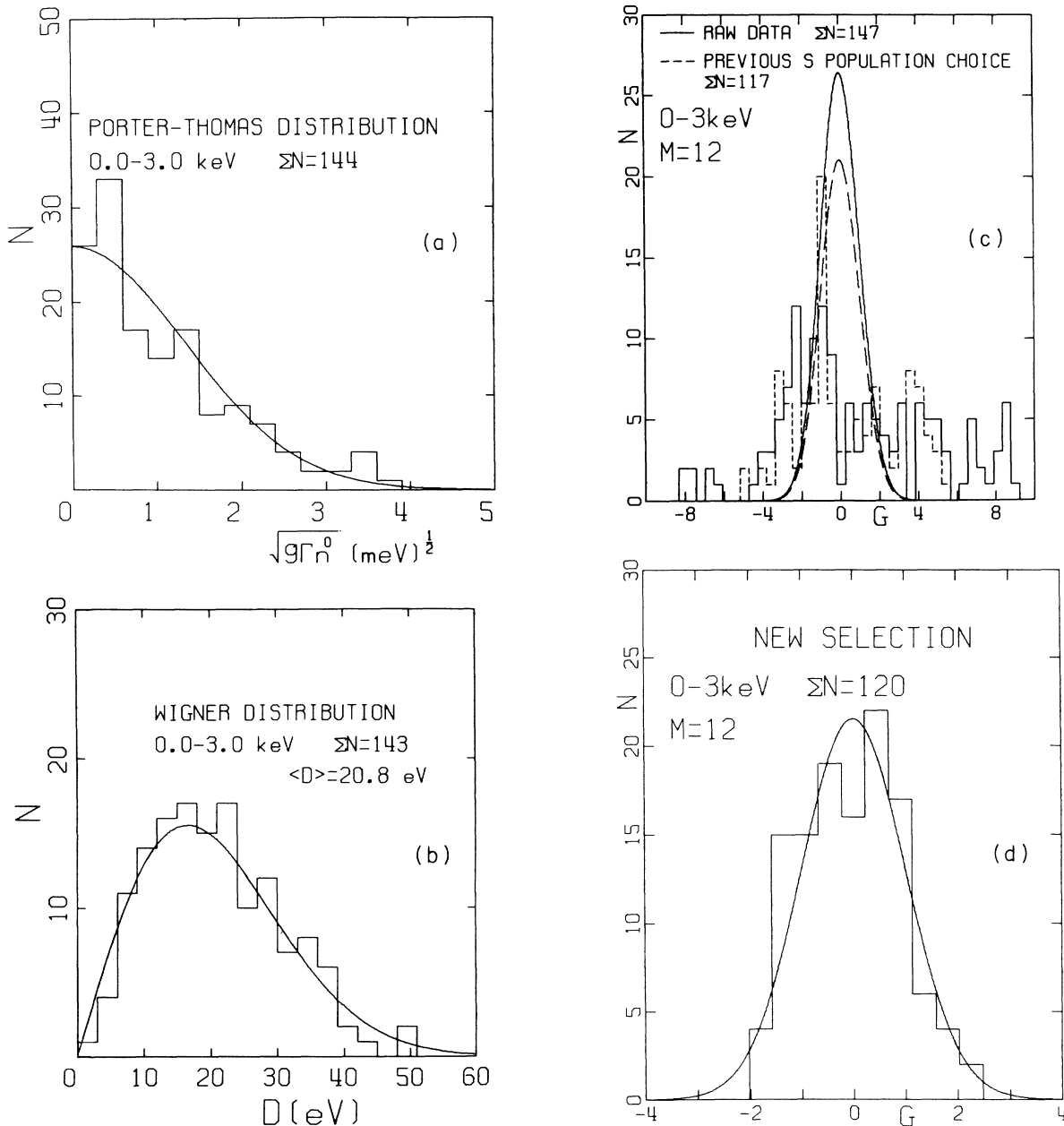


FIG. 6. (a) Histogram of the reduced neutron widths $(\Gamma_n^0)^{1/2}$ ($g=1$) for the newly selected $U^{238} l=0$ population. The Porter-Thomas theory is represented by the smooth curve. (b) Histogram of adjacent level spacings for the newly selected $U^{238} l=0$ population. The smooth curve represents the Wigner distribution. (c) Histograms of G values for the full U^{238} level set (solid line) and the previously selected $U^{238} l=0$ population (dashed line) of IX. The expected behavior is given by the smooth curves. (d) Histogram of G values for the newly selected $U^{238} l=0$ population along with the theoretical O.E. distribution (smooth curve).

These spurious "levels" were removed from the population levels. We also noted that the two levels at 10.2 and 90.0 eV were assigned as being p levels via a Bayes-theorem test by the Argonne Group¹¹ who were the first to emphasize that many of the observed U^{238} levels below 200 eV were probably p levels. Only levels observed experimentally were retained in the new set of levels. The only exception was a level introduced at 1870 eV. A level in this region was strongly required by the F statistic and also implied by the Δ statistic. With the "virtual" level at 1870 eV included, the F statistic in this energy region (see Table IV) is ~ 1 S.D. below the expected value. If an 1870-eV level is not added, a group of F values near 1900 eV is more than 2 S.D. below the average value of F , and there is an asymmetry of the experimental histogram. In addition, if a level is not added at 2870 eV, the experimental value of Δ is increased from 0.417 to 0.676 (the expected value is 0.497 ± 0.11). This provides an interesting demonstration of how sensitive the value of Δ can be to the presence or absence of a single strategically located level.

The PT distribution was crucial for determining the expected number of small resonances. This was implied by the distribution of the stronger s resonances labeled with \dagger in Table IV, which are unlikely to be other than true levels, just on the basis of their Γ_n values.

The final $l=0$ population was required to be consistent with all of the statistical tests. A comparison of the new U^{238} s -population selection with the predictions of the different tests is presented in Figs. 6(a)–6(d). Figure 6(a) shows a comparison with the PT distribution. Similarly, in Fig. 6(b) the histogram of adjacent level spacings is shown along with the Wigner distribution. Histograms of the experimental G values for both the old full U^{238} level set (solid line) and the previously chosen U^{238} s population (dashed line) of IX are shown in Fig. 6(c). The smooth curves represent the expected behavior. Figure 6(d) shows the histogram of experimental G values for the newly selected s population along with the expected behavior (smooth curve). In Table IV are listed the G values found for the old full U^{238} level set of IX, and the newly chosen U^{238} s population. The symbols P, F, N, *, and \dagger have the same meaning as for Table III. The symbol Q to the left of a resonance energy indicates that level was previously reported to be p or spurious. A careful investigation of this table will show what changes have been made. The experimental values of the Δ statistic for the old full U^{238} level set and the new $l=0$ population choice are 9.74 (expected value 0.51) and 0.417 (expected value 0.497), re-

spectively (Table V). Similarly, the old and new values of $\rho(S_j, S_{j+1})$ are -0.006 ± 0.076 and -0.255 ± 0.081 . The new best estimate of $\langle D \rangle$ is 20.8 eV for s levels, with 2% over-all uncertainty. The concluding remarks made previously about thorium apply here also.

The present assignment of weak levels as s or p permits an estimate to be made of the p strength function. An example of this is given in I for Er^{168} , where S_1 for this target nucleus was determined after a selection of the weak s population was made. The p strength functions and other quantities of interest will be published when the full analysis of the more recent (1970) Th^{232} and U^{238} data is completed.

For completeness, we show in Fig. 7 the values of $\sigma(k)$ vs k , the S.D. of the level spacing distribution for levels having k levels between them, for our Th^{232} and U^{238} final s -population choices. This statistical-test display was originated by BF⁶ and is discussed in more detail in I, where

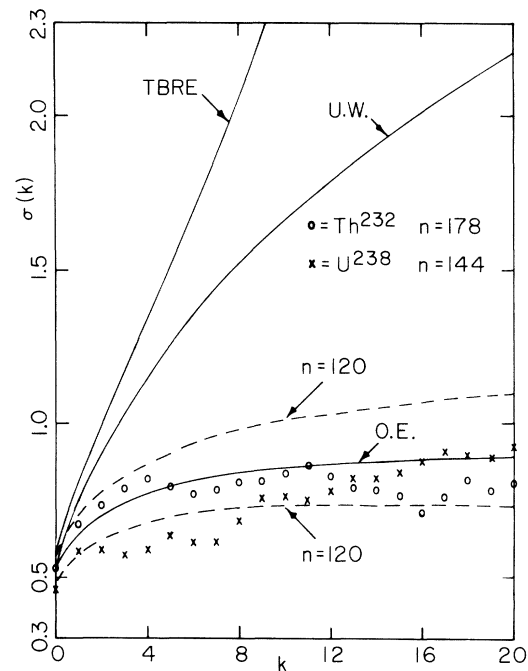


FIG. 7. Plot of $\sigma(k)$ vs k for the new s -level population choices for Th^{232} and U^{238} . Here $\sigma(k)$ is the standard deviation of $S(k)$, the spacing for levels which have k levels between them, in units of $\langle S(0) \rangle$. The O.E. 10 and 90% limits, as well as the O.E. mean, were determined by Monte Carlo type calculations for which $n(\max) = 120$. The corresponding curves for $n = 178$ and 144 (not shown) would be a little closer to the mean than for $n = 120$. The U.W. and Bohigas-Flores TBRE cases (Ref. 6) are shown for comparison.

it is applied to the Er s -population choices. The references are given in I. The results for our s -level population selections for Th²³² and U²³⁸ are in good agreement with the O.E. theory, but not for a U.W. set, nor for the BF TBRE calculation results.

The detailed statistical analysis described above was carried out by H. I. Liou and H. S. Camarda. The level-parameter analysis of the more recent Columbia neutron velocity spectrometer Th²³² and U²³⁸ data is being carried out by F. Rahn.

ACKNOWLEDGMENTS

We would like to thank Professor Freeman Dyson for permitting us to use his F statistic before publication and for a close reading of this manuscript. His encouragement and advice during this work are sincerely appreciated.

Professor Rainwater deserves special thanks for his thorough review of this paper, his incisive remarks, and pithy comments. We also thank Dr. G. Hacken, Dr. M. Slagowitz, and Dr. S. Wynchank for useful discussions.

*Research supported in part by the U. S. Atomic Energy Commission.

†Present address: National Bureau of Standards, Gaithersburg, Md.

¹H. I. Liou, H. S. Camarda, S. Wynchank, M. Slagowitz, G. Hacken, F. Rahn, and J. Rainwater, preceding paper Phys. Rev. C 5, 974 (1972).

²C. E. Porter and R. G. Thomas, Phys. Rev. 104, 483 (1956).

³E. P. Wigner, in Proceedings of the Canadian Mathematical Congress, 1957 (unpublished), p. 174; Columbia University Report No. CU-175, T. I. D. -7547, 1957 (unpublished), p. 49.

⁴F. J. Dyson and M. L. Mehta, J. Math. Phys. 4, 701 (1963).

⁵J. E. Monahan and N. Rosenzweig, Phys. Rev. C 5, 1078 (1972).

⁶O. Bohigas and J. Flores, in Proceedings of the International Conference on Statistical Properties of Nuclei, Albany, New York, 1971 (to be published).

⁷J. E. Monahan and N. Rosenzweig, Phys. Rev. C 1, 1714 (1970).

⁸Unpublished, private communication.

⁹J. B. Garg, J. Rainwater, J. S. Petersen, and W. W. Havens, Jr., Phys. Rev. 134, B985 (1964).

¹⁰P. Ribon, Ph.D. thesis, Universite de Paris, 1969 (unpublished).

¹¹L. M. Bollinger and G. E. Thomas, Phys. Rev. 171, 1293 (1968).

Further Measurements of Gamma Transitions in Spontaneous-Fission Fragments of ²⁵²Cf†

F. F. Hopkins, J. R. White, G. W. Phillips,* C. Fred Moore, and Patrick Richard

Center for Nuclear Studies, University of Texas, Austin, Texas 78712

(Received 1 November 1971)

γ rays in the range from 150 to 1000 keV, following the spontaneous fission of ²⁵²Cf, are observed with a 20-cm³ Ge(Li) detector [full width at half maximum (FWHM) 3.5 keV at 356 keV] in coincidence with K x rays from the fission fragments, observed with a 0.14-cm³ Ge(Li) detector (FWHM 350 eV at 31 keV). Twenty-one 1024-channel γ -ray spectra were accumulated and sorted by computer, corresponding to windows set on K x rays from Zr, Nb, Mo, Tc, Ru, Rh, Pd, Ag, Sb, Te, I, Xe, Cs, Ba, La, Ce, Pr, Nd, Pm, Sm, and Eu. In conjunction with previous work, this data allowed both mass and charge assignments to be made for about 90 of the observed transitions. Relative yields for certain γ rays in self-gated spectra, those for which both x ray and γ ray originated from the same isotope, have been measured and compared with predictions based on previous work.

I. INTRODUCTION

The body of knowledge concerning the fission fragments formed in the spontaneous fission of ²⁵²Cf has been supplemented to a large extent in recent years by studies of γ transitions and internal-conversion transitions in prompt and β -decay

products.¹⁻⁹ X-ray- γ -ray and x-ray-internal-conversion-electron coincidence experiments allow the Z values of the decaying fragments to be determined and in conjunction with mass coincidence experiments allow specific isotope determinations to be made. The low-energy transitions in these fragments have received a considerable